Journal of the Korean Society of Marine Engineering, Vol.29, No.3, pp.260~274, 2005(ISSN 1226-9549)

An Experimental Study on Swirling Flow with Heat Transfer in the Horizontal Circular Annuli

Tae-Hyun Chang†

(Manuscript : Received FEB 15, 2005 ; Revised MAY 12, 2005)

Abstract : An experimental investigation was performed to study the characteristics of turbulent swirling flow in the cylindrical annuli. The swirl angle measurements were performed by flow visualization technique using smoke and dye liquid. By using the particle image velocimetry method, this study has found the time-mean velocity distribution and turbulent intensity with swirl for Re=20,000, 30,000, 50,000, and 70,000 along longitudinal sections. The results appear to be physically reasonable.

Other experimental study was performed to investigate heat transfer characteristics of turbulent swirling air flow in axisymmetric annuli. The static pressure, the local air flow temperature, and the wall temperature with decaying swirl were measured by using thermocouples and the friction factor and the local Nusselt number were calculated for Re=30,000, 50,000 and 70000. The local Nusselt number was compared with that obtained from the Dittus-Boelter equation with swirl and without swirl, respectively. The results showed that the swirl enhances the heat transfer at the inlet and the outlet of the test tube.

Key words : Annuli, Swirl angle, Concave tube, Convex tube

Nomenclature

A : Cross Section area of the test tube [m^2]
C_p : Specific Heat at Constant Pressure [kJ/kgK]
D : $(d_0 - d_i)$[mm]
d_0 : The annulus concave diameter [mm]
d_i : The annulus convex diameter [mm]
f : Friction factor for fully-develope flow
f_s : Friction factor for swirl flow
h : Heat transfer coefficient [W/mK]
k : Thermal conductivity [W/mK]
L : Length of the swril chamber [m]
Nu : Nusselt number
Nu_s : Nusselt number for swirling flow
P : Fluid pressure [Pa]
P_0 : Atmosperic pressure [Pa]
P_r : Prandtl number
P_s : Static pressure [Pa]
P_v : Total pressure [Pa]

† Corresponding Author(Division of Mechanical and Automation Engineering, Kyungnam University)
E-mail : changtae@kyungnam.ac.kr, Tel : 055)249-2613

R_c : (R_o/R_i)
Re : Reynolds number
R_i : Radius of the convex tube [mm]
R_0 : Radius of the concave tube [mm]
S : swirl intensity

$$S=\frac{1}{R}\left[\int_0^r uwr^2 / \int_0^r u^2 r dr\right]$$

T : Local air temperature [℃]
T_i : Wall temperature on the convex tube [℃]
T_r : Room air temperature [℃]
T_w : Wall temperature [℃]
U : Time averaged axial velocity [m/s]
V : Time averaged radial velocity [m/s]
u : luctuating velocity [m/s]
v : luctuating velocity [m/s]
w : luctuating velocity [m/s]
X : Axial coordinates [mm]
y : Radial position [mm]

Greek Symbols

ρ : Density [kg/m^3]
ν : Kinetic viscosity [m^2/s]
τ_w : Wall shear stress [N/m^2]
θ : Swirl angle [°]

1. Introduction

The flow in a cylindrical annuli, which has been widely utilized in boiler feed water heaters, heat exchangers between sea water and cooling water, tubular type heat exchangers, cyclotron and in cooling the rotor and stator of motors and generators, has been investigated extensively.

The one who attempt to study the field for the first time was Rothfus[1], who considered the friction coefficient and velocity profiles of air flow in the tube. Next year, he formulated concepts on turbulent intensity and the Reynolds stress. Using a Pitot tube and hot wire anemometer, Brighton et al.[2] investigated the mean velocity, turbulent intensity, and Reynolds stress of water in the range of Re=46000 to 327000.

Alan[3] measured the friction coefficient and velocity profile of water flow through the test tube for Re=6,000 to 9,000, which had a ratio of R/r=2.88 to 9.37.

Additionally, Tuft et al.[4] investigated the Nusselt number of water flow through a cylindrical annuli in Re=41~465 by the finite difference and experimental methods, and Molki et al.[5] measured the Nusselt number of air flow through an inner helical convex tube in Re=500~1250 by the naphthalene sublimation method. In the beginning of the 21st century, Garimella et al.[6] reported on the tube friction coefficient of water for Re=310~1000 in a scroll annuli with a groove and also the Nusselts number by making use of the LMTD (Log Mean Temperature Difference) method. The tube friction coefficient of the turbulent flow was 10 times greater than that of laminar flow and the Nusselts number was 4~20 times greater than that of the flow.

In the early investigations into the influence of swirl on fluid flow, Chigier et al.[7], Scott et al.[8], Milar[9], and Clayton et al[10] studied about the swirl flow through a cylindrical annuli by measuring velocity profiles and pressure losses and applying the numerical analysis method.

Recently, Chang et al.[11] measured the velocity profiles and Reynolds stress in the horizontal cylindrical tube by using the Particle Image Velocimetry method.

The study on the heat transfer coefficient of several heat exchangers has been increased by enlarging the area of heat transfer, introducing artificial illuminators and coils, by protruding fins or making grooves in the tube.

Thus, this study was performed to investigate the characteristics of swirl flow with heat transfer in the horizontal annuli having a radius ratio of Rc=3.0. To measure swirl angle, the time mean velocity by PIV technique, the static pressure, the local flow temperature and the tube wall temperature of swirl and non-swirl flow of Re=30,000 and 80,000 under a uniform heat flux, and to find out the Nusselts number and contribute to the compact and economical design of heat exchangers.

2. Experimental Apparatus

Fig. 1 shows the layout of the experimental apparatus used in this study. The experimental rig were manufactured from an acryl tube for flow and a cupper tube for the heat transfer measurement. A concave tube diameter of 150 mm and a length of 3,000 mm, a convex tube diameter of 50 mm and a length of 3,000 mm, and a stainless tube with an inner diameter of 50 mm and a length of 4,000 mm were used throughout this experiment. The swirl generator was installed at the entrance of the test tube. Because Taurus Controls Ltd. certified their multi-pitot tube for the non-swirling flow but not for the swirling flow, a honeycomb was installed in the front of the test tube, and so it was possible for this tube to be used in the swirling flow.

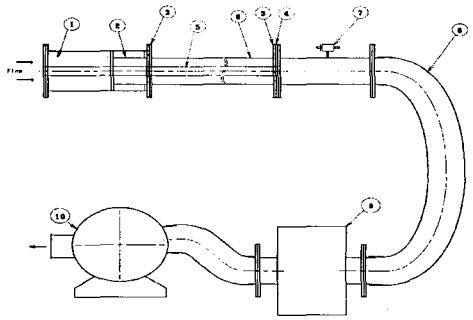

① Swirl chamber	② Swirl generator
③ Teflon flange(for concave tube)	④ Teflon flange (for convex tube)
⑤ Convex tube (PVC tube)	⑥ Test tube (Concave, Copper)
⑦ Multi pitot tube(TORBAR 301)	⑧ Flexible hose
⑨ Air chamber(Φ600×H1,000mm)	⑩ Recirculation Pump(220V,5HP)

Fig. 1 Experimental apparatus for swirling flow

The swirling generator was fabricated using an acryl tube with an outer diameter of 150.0 mm, in which eight holes with a diameter of 3.2 mm were drilled at 45° intervals from the outer to inner the tangential direction. In order to adjust the swirling intensity, the swirling generator was designed to be able to move in the swirl chamber.

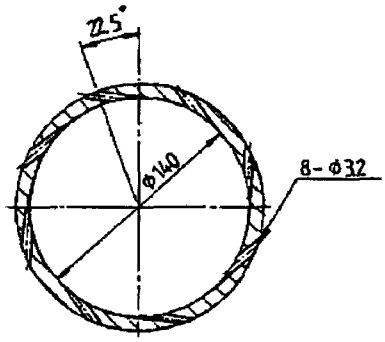

Fig. 2 Cross section view through the swirl generator.

For the non-swirling flow experiment, the swirling generator and swirl chamber were dismantled and connected by a guide tube having the same diameter.

2.1 Experimental method and PIV System

In order to determine some of the swirl flow characteristics of the swirl flow induced by the swirl chamber used in this investigation, the flow visualization experiments were carried out first using smoke and dye liquid.

The velocities were measured using the 2-D PIV technique, and the swirl motion of the fluid was produced by a tangential inlet condition. The algorithm used was the gray level cross-correlation method (Kimura et al. 1986)[12]. An Ar-ion laser was used and the light from the laser (500 mW) passes through a probe to make a two-dimensional light sheet. In order to make coded images of the tracer particles on one frame, an AOM (Acoustic-Optical Modulator) was used. The AOM controller was synchronized with the camera and a carrier signal was sent to the AOM unit at 100 MHz, which enabled the AOM system to work as an electric shutter, as shown by Kobayashi et al[13].

The images taken through the camera were captured with a frame grabber (DT3155) and converted into 8 bit levels on the host computer. The particles used in the experiment were nylon 12 (50 m). For these field images, the velocity vectors were obtained by using the PIV algorithm. The calculation time on the host computer (Pentium 550 MHz) was about 3 minutes in the case of the grid of 3570, the radius for the searching area was set to 25 pixels, the size for the correlation area was set to 3232 pixels. In order to eliminate error vectors, an error vector elimination method based on the continuous flow condition was adopted.

In order to prohibit the refractive effects of the circular tube on the results, a square box was installed, which recovered the refracted light waves from the visualized section of the flow. Figure 3 show the diagram of the PIV system used in this experiment.

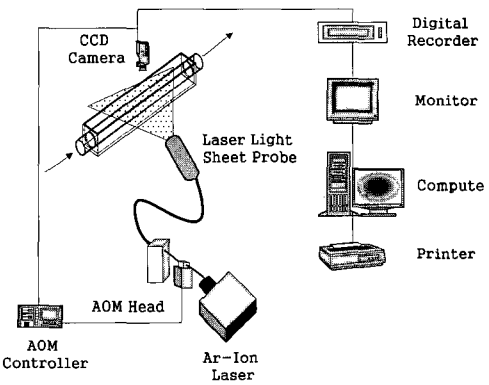

Fig. 3 Schematic arrangement of the PIV system

2.2 Heat transfer apparatus

The experimental apparatus for heat transfer is identicaly same in size in this study with swirl and without swirl. A concave tube, with an inner diameter of 150 mm, and a length of 3000 mm, and a copper tube with the outer part uniformly wound at the space of 12 mm with a heating coil (Pyrotenax Ltd.) of 2.6 kW, 240 V, were fabricated to uniformly transfer heat to the fluid. The entrance flange of the test tube was made of bakelite, but the exit flange, taking thermal expansion into consideration,

was made of Teflon. Sixty-four thermocouples were installed at a space of 90°in 16 test tube sections, that is, four thermocouples in a section. In order to measure the inside flow temperature of the test tube, 16 thermocouple ports were installed onto the surface of the test tube, which was wrapped with a glass wool blanket of more than 50 mm thickness.

A voltage regulator was installed to adjust the requirement of a 240 V heating coil. A transformer was prepared to measure voltage and current to find heat flux value. Meanwhile, a multi-Pitot tube was installed at the end of tube to identify the Reynolds number of air, from which the fluid velocity was to be determined. The rpm of the fan motor was controlled. The local flow and wall temperature of the tube were measured by thermocouples to determine the heat applied to the fluid.

3. Results and Discussion

3.1 Swirl Angle Measurement

Several calculations have been performed based on experimental results in order to evaluate the swirl number and define the ratio of angular momentum to linear momentum flux. The 2D PIV technique is used for velocity measurements. Therefore, in the present study, the Reynolds number rather than swirl number is used.

One of the primary objectives of this research was to measure the swirl flow angle along the test tube for different Reynolds numbers. The Reynolds number for these measurements ranged from 60,000 to 100,000 with L/D=0 to 4.

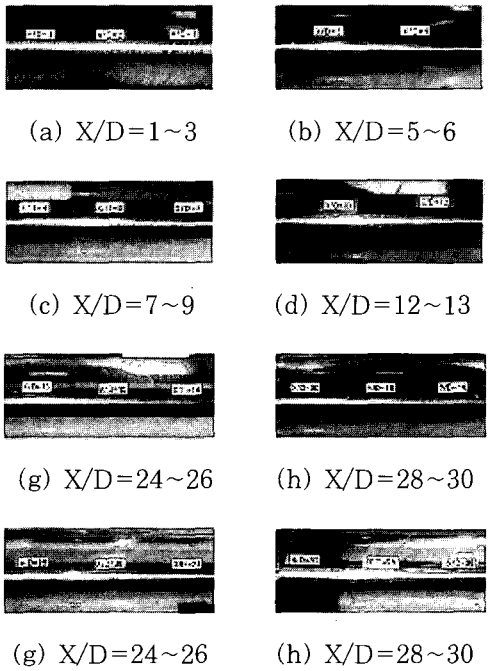

(a) X/D=1~3 (b) X/D=5~6

(c) X/D=7~9 (d) X/D=12~13

(g) X/D=24~26 (h) X/D=28~30

(g) X/D=24~26 (h) X/D=28~30

Fig. 4 Swirl angle distributions along the tube using smoke for Re=60,000 at L/D=0

During the flow visualization test, it was observed that some of the water-based liquid used to generate the smoke had condensed. This was deposited on the inside of the concave tube wall in the form of droplets that followed the path of the swirl flow.

Similar results were obtained by Sparrow[14] who injected an oil lamp black mixture onto white plastic, self-adhering contact paper positioned inside the tube. By removing the paper, the angle made by the flow relative to the tube axis could be measured. In the present experiment, these angles were evaluated by placing a clear plastic sheet over the outside of the concave tube, tracing the streak lines,

and then measuring the angle using a method similar to that of Sparrow[14]. The movement of the droplets was, of course, due to the shear stress exerted by the flow at the tube wall. The flow angles were measured at eight pre-selected locations along the length of the test section tube.

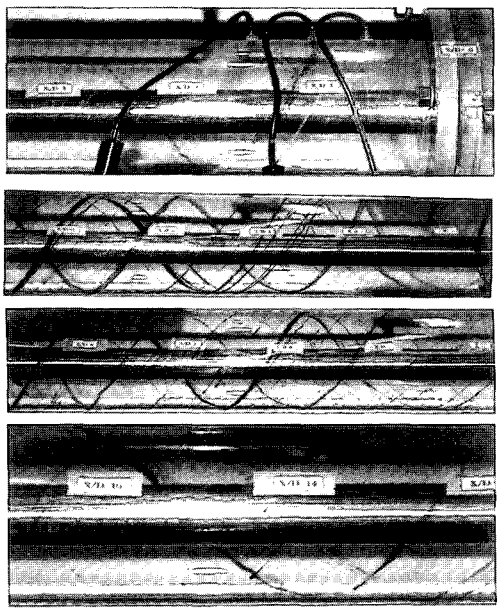

Fig. 5 Swirl angle distributions along the test tube by using dye liquid for Re=80,000 at L/D=4 and X/D=1~15.

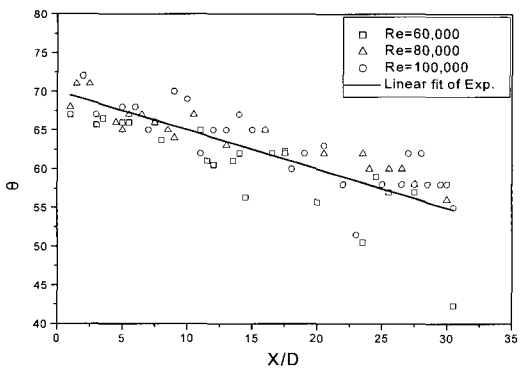

Fig. 6 Comparisons of swirl angle for Re=60,000, 80,000 and 100,000 at L/D=0.

The results obtained using smoke for Re=60,000 are shown in Fig. 4. In each figure, flow angles are plotted as a function of X/D for both the extreme plenum chamber lengths (L/D=0 and 4). Fig. 5 shows the swirl angle using the dye liquid for Re=80,000. Fig. 6 illustrates the decay of the swirl angle along the test tube for Re=60,000~100,000 and hence the ratio reduction of the tangential and axial shear stresses. The swirl flow starts with an angle of 70° with respect to the axial direction and decays to 55° at a location close to the end of the test section tube. This angle would have been zero in the case of a pure axial flow. Inspection of the figures shows that decreases with X/D, as shown earlier, and that increases in Reynolds number are accompanied by increases in the swirl angle. At any fixed value of X/D and Reynolds number, the swirl angle increases as L/D is increased and as the swirl intensity is increased (i.e. L/D=0 to 4).

The fitted versus X/D equations were of the form

$$\theta = 64.285 + (7.216 * 10^{-5})Re - 0.633(L/D) - 0.504(X/D) \quad (1)$$

This finding was further confirmed a lot of conditions with Reynolds number, X/D and L/D using smoke and dye liquid.

3.2 Velocity Profiles

Fig. 7 shows the time mean velocity vector for Re=20,000 along the test tube. The velocity vector is indicated as a negative value near the convex tube, and then the vector is changed to a positive

vector after X/(D-d)=7 with a decaying swirl intensity. However, a strong vector was observed near the concave tube, and in particular, uniform velocity vectors are observed at y/(R-r)=0.7~0.75. The results appeared to be for a similar phenomenon that is not related to Reynolds number.

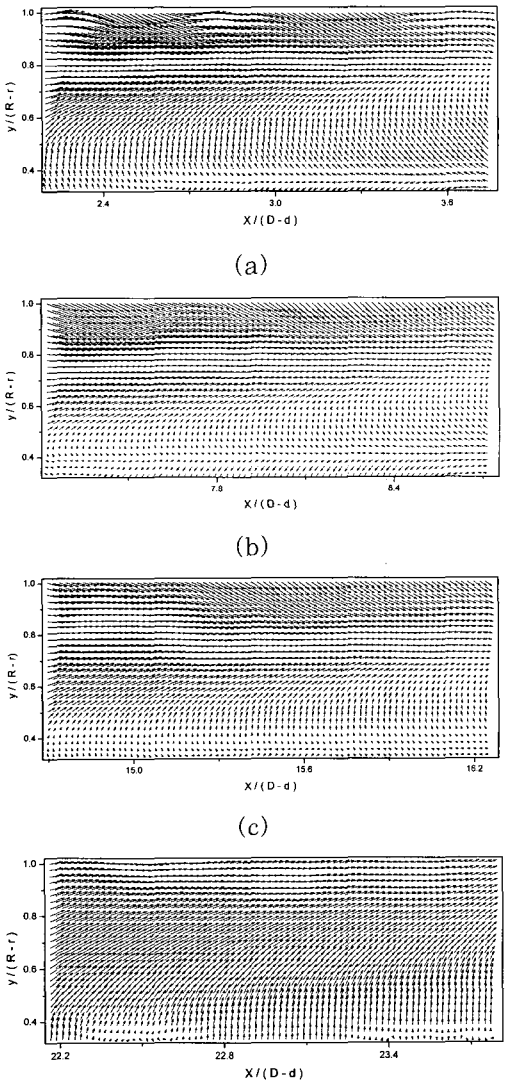

Fig. 7 Time-mean velocity vectors with swirl along the test tube for Re=20,000 at (a) X/(D-d)=3.0, (b) 8.0, (c) 15.5 and (d) 23.0

In addition, these gradually disappeared along the test tube. These aspects are related to the decaying tangential velocity with swirl along the test tube. Fig. 8 depicts the local axial velocities at X/(D-d)=3, 5.5, 8, 13, 15.5, 18, 23 and 25 for Re =20,000 and Re=40,000 that were calculated from the vector shown in Fig. 7.

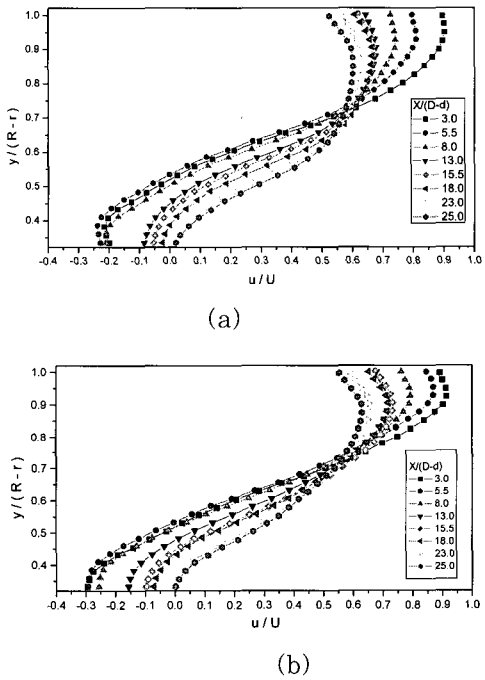

Fig. 8 Time-mean axial velocity profiles with swirl along the test tube for (a) Re=20,000 and (b) Re=40,000.

The local axial velocities in Figure 8 show negative velocity profiles at X/(D-d)=3~25 along the convex tube. The negative velocity region was increased according to increasing Reynolds number.

However, there is a neutral point for equal velocity at y/(R-r)=0.7~0.75, and the highest velocity near y/(R-r)=0.9.

The maximum velocity point moved to the concave tube by increasing the Reynolds number, but the point also moved to the convex tube by the swirl flow decaying along the test tube. Until now, accurate measurement of the velocity near the wall of a test tube was difficult using hot wire anemometry and LDV.

Unlike in previous research on swirling flow, negative vectors and velocities were observed near the convex tube along X/(D-d)=3~25. Phenomena such as these are similar to those associated with the swirling flow in a horizontal circular tube; however, the velocity gradient is smoother than that of a single tube with a swirl flow.

Tangential velocity is thought to have quickly decayed through the concave and convex walls.

3.3 Turbulence Intensity Profiles

Fig. 9 depicts the contours of axial turbulence intensity profiles calculated from the vectors for Re=20,000. These intensities show maximum value near the concave wall and at y/(R-r)=0.5. The former indicates the highest axial turbulence intensity near the concave wall as influenced by tangential velocity and the latter becomes associated with the boundary of the recirculating zone. These results were observed due to different velocity gradients existing next to each other near the convex wall.

However, the axial turbulence intensity was minimal at y/(R-r)=0.8~0.9 and near the convex tube wall. This phenomenon was observed in association with the negative axial velocity.

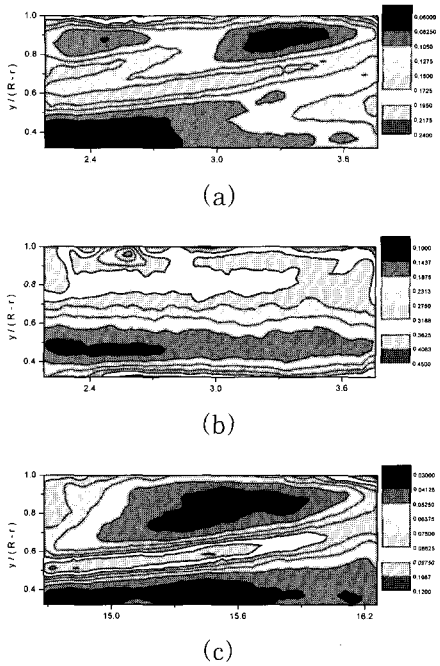

Fig. 9 Contours of axial turbulent intensity(u) along the test tube with swirl at (a) X/(D-d)=3.0, (b) 15.5 and (c) 25.0 for Re=20,000

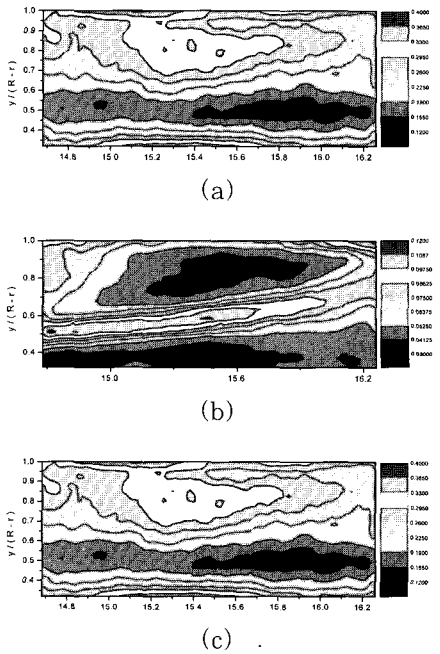

Fig.10 Contours of radial turbulent intensity(v) along the test tube with swirl for Re=20,000 at (a) X/(D-d)=3.0, (b) 15.5 and (c) 25.0

The contour of radial turbulence intensity profiles are plotted in Fig. 10. Unlike axial turbulence intensity, these intensities show strong values near the concave and convex tube walls. In addition, these intensities revealed an interesting phenomenon, the lowest radial turbulence intensity was observed near the boundary of the recirculating zone, y/(R-r)=0.5. The results showed a similar phenomenon, although the Reynolds number continued to increase. This is thought to be associated with the strong swirl flow in the horizontal annuli.

3.4 Static Pressure Distributions

The static pressures for Re=40000 to 75000 at the 14 locations X/D=0.5, 0.8, 1.5, 2.0, 4.0, 5.0, 6.1, 7.3, 8.0, 10.2, 14, 18, 24, 26.5 were measured at the concave and convex tube by inclined Manometer (Air flow, MK5) before performing the heat transfer experiment.

Furthermore, 14 numbers of 2 mm static pressure holes were drilled into the concave tube. Then, 2 mm tubes were installed and connected to the Manometer, which could measure the static pressure of the fluid. Two mm static pressure holes were pierced and one end of the 2 mm copper tubes was connected to the inclined manometer, and the static pressure of air was measured.

At this moment, y-direction locations between the concave and convex tubes were being prepared to be precisely coincide with a transmitter so that the experiment could be performed.

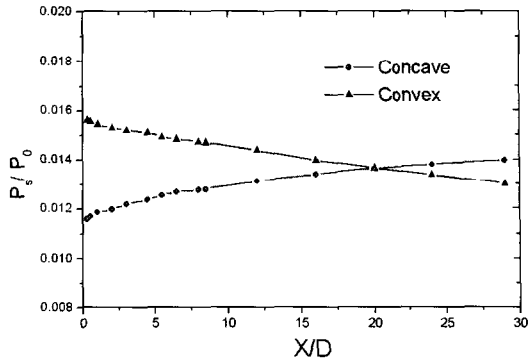

Fig. 11 Distributions of the static Pressure along the test tube with swirl for Re=40,000.

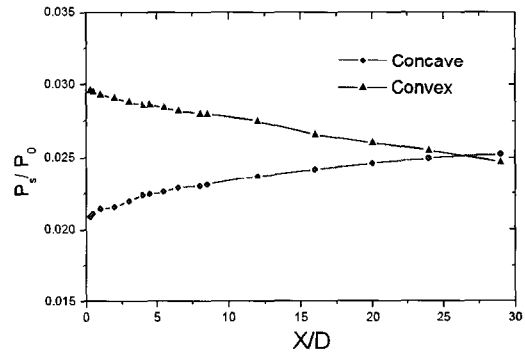

Fig. 12 Distributions of the static Pressure along the test tube with swirl for Re=75,000.

Fig. 11 and Fig. 12 show the static pressures of the fluid for Re=40000~75000, which was flown through the concave and convex tubes.

The static pressure of the wall was high at the test tube entrance, but gradually decreased along the tubes (increased in the Fig.11 and Fig. 12. This appeared to be high at the test tube entrance by the tangential velocity component of the swirling flow, and the static pressure also increased. This static pressure gradually decreased as the swirling flow decreased along the tube.

But for the convex tube wall, the static

pressure was low at the tube entrance but gradually increased along the tube (decreased in Figure).

Near the tube entrance, the negative velocity zone usually formed in the direction of the convex wall due to the swirl intensity. It was unusual that there was a cross point of two static pressures (as they were swirl-decayed). In Re=40000, it was at about at X/D=20, but in Re=75000, it was at about X/D=27. This result implied that when the Reynolds number increases, the point moves away from the entrance of the annuli. This was thought to have come from that the swirl intensity was a function of the Reynolds number.

3.5 Friction Factor

Using equation (2), the tube friction factor of the swirl and non-swirl flow was derived. In the fully developed zone, the friction coefficient was applied as the Blasius' equation.

$$f = \frac{\tau_w}{0.5\rho U^2} \qquad (2)$$

The friction factors of the concave and convex tubes, respectively, were calculated from information in the static pressure distribution chart of Figs.12 and compares the friction factor(fs/f) of the swirl flow for Re=40,000 in the concave tube with that derived for the horizontal short tube by Sparrow et al.[14].

It is likely that in the swirling flow, this result came from the tangential velocity component. The result was compared with that from the Sparrow's work[14]. His Reynolds number was 43,500 with swirling flow of the horizontal single tube.

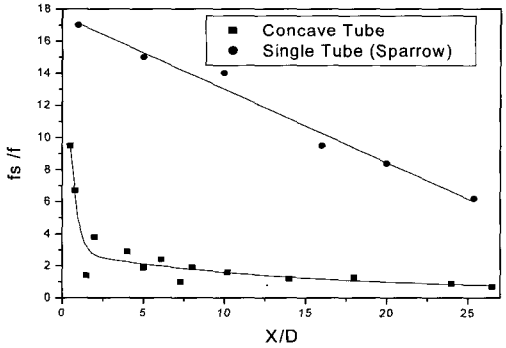

Fig. 13 Comparisons of the friction factor on the concave tube and the single tube with swirl for Re=40,000

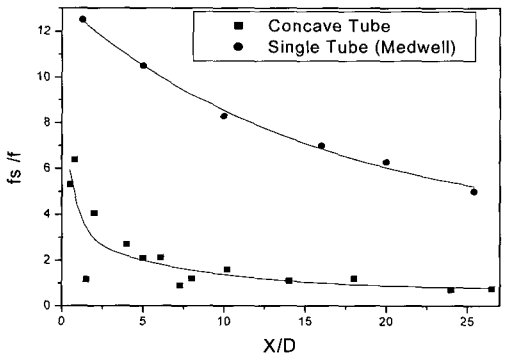

Fig. 14 Comparisons of the friction factor along the test tube with swirl for Re=75,000

The value in the entrance of the test tube was shown to be 1.7 times higher than that of the annuli; and in the end of the tube it was 6.3 times higher.

The comparison of the fs/f of the annuli for Re=75,000 with that of Medwell et al.[15] are given in Fig. 6. Medwell's[15] results also appeared to be about 2 times higher in the tube entrance and 5.2 times higher in the tube end than in the annuli. As it were, the fs/f in the swirling flow was shown to be 1.7~2.0

times higher in the test tube entrance and 5.2~6.3 higher in the tube end than in the annuli. This phenomena was thought to have occured due to the swirling flow in the annuli to accelerate the nullification of the swirling flow from the friction of the concave and the convex tube.

4. Heat Transfer Results

4.1 Local Air Temperature Distributions

Fig. 15 and Fig. 16 include the local air flow temperature(T/Tr) of the non-swirling flow at Re=30000 and 70000 respectively.

For the non-swirling flow, the air temperature at Re=30,000 was consistent when X/D=0.5~4.5, y/(Ro-Ri)=0.7, but as X/D increased, T/Tr gradually increased. Near the concave tube wall it sharply increased and appeared higher as the Reynolds number decreased. Meanwhile the local temperature distribution of Re=30,000 near the convex tube was 1.0~2.3 at y/(Ro-Ri)=0.325 but smaller when Reynolds number increased, and at Re=70,000 the local temperature distribution appeared as y/(Ro-Ri)=1.1~1.7. It was thought that as the Reynolds number was low, the temperature distribution near the convex tube had some variations, but as Reynolds number increased, it was smaller owing to the axial velocity increment. It was shown that the fluid temperature decreased, having no relation with the change of the Reynolds number. But, the dimensionless temperature(T/Tr) was decreased at X/D=29.0~29.5 with no relation with the change of Reynolds number.

It likely come from the effect of the tube end. This phenomenon also appeared to have no relation with the change of Reynolds number.

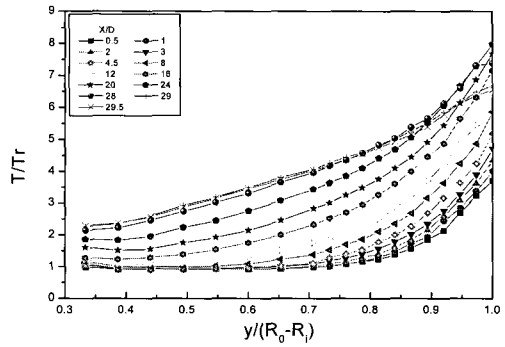

Fig. 15 Distributions of Tempeture Profile without Swirl across the Test Tube for Re=30,000

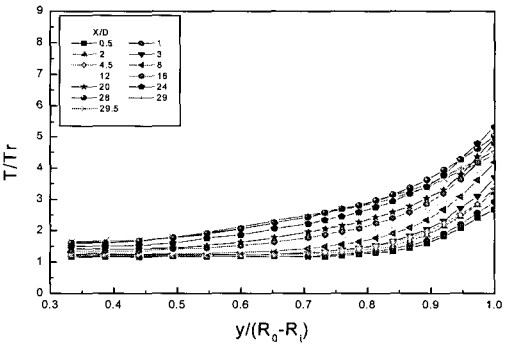

Fig. 16 Distributions of Tempeture Profile without Swirl across the Test Tube for Re=70,000

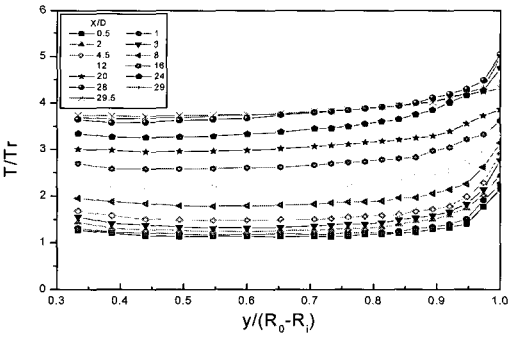

Fig. 17 Distributions of Tempeture Profiles with Swirl across the Test Tube for Re=30,000

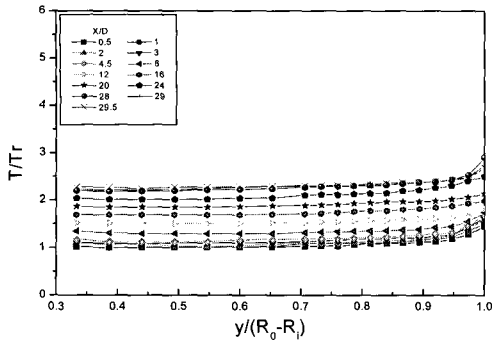

Fig. 18 Distributions of Tempeture Profiles with Swirl across the Test Tube for Re=70,000

Fig. 17 and Fig. 18 show the local fluid temperature (T/Tr) with swirling flow, which appeares to be consistent to y/(Ro-Ri)=0.325~0.9 for Re=30,000 and different from the non-swirling flow. Except for the near tube wall, the temperature of y direction of the test tube appeared to be consistent even though X/D increased.

The temperature gradient near the tube wall sharply increase in the small range compared with non-swirling flow. The tangential velocity component of the swirling flow was regarded to transfer more energy from the tube wall to the fluid than that of the non-swirl flow. In addition, when the Reynolds number increased, the local temperature near the convex tube decreased and the temperature range apparently decreased compared with non-swirling flow so that in Re=30,000, the range was 1.2~3.65 at y/(Ro-Ri)=0.325 but in Re=70,000, 1.0~2.3. It was also considered that the energy from the heated wall was transferred to the near convex tube wall with the fluid mixture caused by the tangential velocity of the swirl flow.

4.2 Wall and Dimensionless Temperature

Fig. 19 depicts the relation between Reynolds number and the wall temperature (Tw/Tr) of the non-swirling flow. At the tube entrance the wall temperature distribution is shown to steeply increase but after X/D=10, up to 24 it gradually increased. Namely, this range is regarded as the thermally full developed region in the annuli, but after X/D=25 it decreased along the test tube. This phenomenon is the same as the local fluid temperature distribution of the tube end regarded as the effect of the tube end. The wall temperature distribution decreased as the Reynolds number

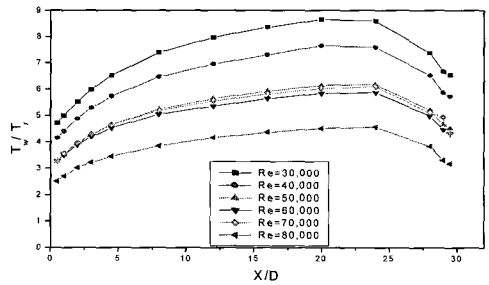

Fig. 19 Comparison of T_w/T_r without swirl for Re=30,000, 40,000, 50,000, 60,000, 70,000 and 80,000

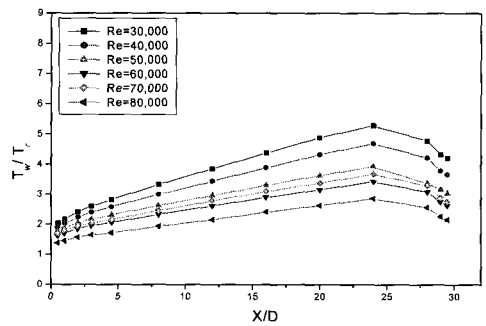

Fig. 20 Comparison of T_w/T_r with swirl for Re=30,000, 40,000, 50,000, 60,000, 70,000 and 80,000

increased. This means more energy from the wall is transferred to the fluid the average velocity increases according to Reynolds number.

Fig. 20 also include the wall temperature in the swirling flow. Tw/Tr of the test tube entrance, which was 2.5~4.6 in the non-swirling flow, was much lower in the swirling flow, 1.3~20. Furthermore, the maximum temperature, which was 8.8 in the non-swirling flow, was very low in the swirling flow as 5.2. It means that the swirl flow transferred more energy from the heated tube wall to the fluid than that of the non-swirling flow. But it is a particular phenomenon that is consistent with the local fluid temperature variation

4.3 Comparisons of Nusselts number with Swirl and without Swirl flow

The fundamental bulk temperature could be calculated from equation (3) and (4), but because it was found out after measuring the local fluid temperature and the axial velocity, the bulk temperature of each zone was calculated by equation (3), and the local Nusselts number was done by equations (5), (6) and (7). Finding out the bulk temperature from the local fluid temperatures of Fig. 15~Fig. 18, and the specific heat and heat transfer coefficient of the fluid, Nusselts number was calculated for swirl flow and non-swirl.

$$T_b = \frac{\int_0^{r_0} \rho 2\pi \, dr \, u \, c_p T}{\int_0^{r_0} \rho 2\pi \, dr \, u \, c_p} \tag{3}$$

$$T_b = \frac{1}{A} \int_A T dA \tag{4}$$

$$dq = m \, C_p d \, T_b \tag{5}$$

$$h = \frac{m \, C_p d \, T_b}{2\pi r \, dx \, (T_w - T_b)_{mean}} \tag{6}$$

$$Nu = hD/k \tag{7}$$

The calculated Nusselts number was compared with the results, which was calculated from the Dittus & Boelter equation. Here, Pr is Prandtl number.

$$Nu = 0.0023 Re^{0.8} \mathrm{Pr}^{0.4} \tag{8}$$

Fig. 21 also includes the comparisons between Nusselts number over the Reynolds number range of Re=30,000~80,000 with swirling flow and without swirling flow. Nusselts number of swirling flow was observed to be 2.0~2.5 times bigger than the one for the non-swirling flow at X/D=10~25. It was also observed to be 2.3~3.3 times bigger at the tube entrance and 3~4 times bigger at the tube end. It is thought that the swirling flow could be more heat transfer by fluid mixing due to tangential velocity.

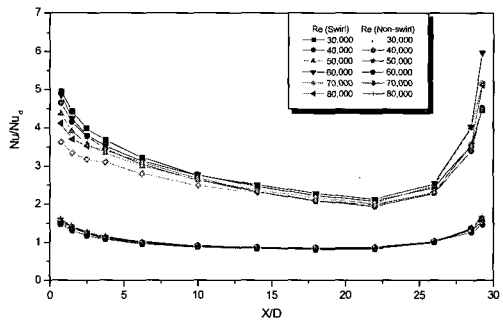

Fig. 21 Comparison of Nusselts number with Swirl and without swirl for Re=30,000, 40,000, 50,000, 60,000, 70,000 and 80,000

It means that the Reynolds Number is a function of swirl intensity so if that Reynolds Number is increased, the tangential velocity is increased and the heat transfer from the heated wall is also increased.

5. Conclusions

The following conclusions were obtained for a cylindrical annuli using flow visualization and PIV techniques in water and air, where the swirling and non-swirling flow moved through a horizontal annuli of air fluid

1. The swirl angle was derived from the following equation using a flow visualization test.

$$\theta = 64.285 + (7.216 * 10^{-5}) Re - 0.633(L/D) - 0.504(X/D)$$

2. The velocity vector had a negative value near the convex tube and then the vector changed to a positive after X/(D-d)=7 with decaying swirl intensity.

3. There were neutral points for equal axial velocity at y/(R-r)=0.7~0.75, and the highest axial velocity was recorded near y/(R-r)=0.9. Negative axial velocity was observed near the convex tube along X/(D-d)=3~23.

4. The axial turbulence intensities showed maximum value near the concave wall and at y/(R-r)=0.5. However, a particular phenomenon was observed when radial turbulence intensities were investigated. The lowest intensity was noted near the boundary of the recirculating zone, y/(R-r)=0.5.

5. The friction factor in the concave tube of the annuli was 1.7~2.0 times lower at the tube entrance and 5.2~6.3 times lower at the exit than those of the single test tube. The fluid temperature distributions fromthe convex to concave tube in the swirling flow was consistent up to y/(Ro-Ri)=0.9. This phenomenon continued as the Reynolds number increased.

6. The Nusselts number of the swirling flow was observed to be 2.0~2.5 times higher than one in the fully developed regions of the non-swirling flow. It was regarded as a phenomenon that owing to the tangential velocity component of the fluid, caused more energy to be transferred from the heated wall in the swirling flow to the fluid than in the non-swirl flow.

7. In the fully developed zone without swirl flow, the Nusselt number was lower than that of Dittus & Boelter equation. However, the swirling flow has no fully developed region.

Acknowledgments

This work is supported by Kyungnam University research fund, 2005.

References

[1] Rothfus, R. R., "Velocity Distribution and Fluid Friction in Concentric Annuli", Ph.D. thesis, Carnegie Institute of Technology, 1948.

[2] Brighton, J. A. and Jones, J. B., 1964, "Fully Developed Turbulent Flow in Annuli", J. of Basic Engineering, pp. 835-843.

[3] Alan, Q, "An Experimental Study of Turbulent Flow Through Concentric

Annuli", Int. J. Mech. Si, Vol. 9, pp. 205-221, 1967.

[4] Tuft, D. B. and Brandt, H., "Forced Convection Heat Transfer in a Spherical Annulus Heat Exchange", J. of Heat Transfer, Vol. 104, pp. 670-677, 1990.

[5] Molki, M., Astill, K. N. and Leal, E., "Convective Heat-mass Transfer in Temperature Region of a Concentric Annulus having a Rotating inner Cylinder", Int. J. Heat and Fluid Flow, Vol. 11, No. 2, 1990.

[6] Garimella, S. and Chritensen, R. N., "Heat Transfer and Pressure Drop Characteristics of Spirally Flute Annulli: Part II Heat Transfer", J. of Heat, Vol. 117, pp. 55-68, 1995.

[7] Chigier, A. N. and Beer, J. M., "Velocity and Static Pressure Distributions in Swirling Air Jets Issuing From Annular and Divergent Nozzle", ASME, J. of Basic Engineering, pp. 788-796, 1964.

[8] Scott, C. J. and Raske, D. R., "Turbulent Viscosities for Swirling Flow in a Stationary Annulus", ASME J. of Fluid Engineering, pp. 557-566, 1973.

[9] Milar, D. A., "A Calculation of Laminar and Turbulent Swirling Flows in Cylindrical Annuli", ASME, Winter Annual Meeting New York Dec. pp. 89-98, 1979.

[10] Clayton, B. R., and Morsi, Y. S. M., "Determination of Principal Characteristics of Turbulent Swirling Flow Along Annuli", Int. J. Heat & Fluid Flow Vol.6, No.1, pp. 31-41, 1985.

[11] Chang, T. H. and Kim, H. Y., "An Investigation of Swirling Flow in a Cylindrical Tube", KSME Int. J., Vol. 15, No.12, pp. 1892-1899, 2001.

[12] Kimura I., Takamori T. and Inoue T., "Image Processing Instrumentation of Flow", Flow Visualization, Vol. 6, No. 22, pp. 105-108, 1986.

[13] Kobayashi, T., Saga, T., and Doh, D., N., "A Three-Dimensional Simultaneous Scalar and Vectore Tracking Method", Proc. Int. Workshop on PIV. Fukui, Japan, pp. 33-43, 1995.

[14] Sparrow, E. M. and Chaboki, A., "Swirl-Affected Turbulent Fluid Flow and Heat in a Circular Tube", J. of Heat Transfer ASME, Vol. 106, pp. 766-773, 1984.

[15] Medwell, J. O., Chang, T. H. and Kwon, S. S., "A Study of Swirling Flow in a Cylindrical Tube", Korean J. of Air-Conditioning and Refrigeration Engineering, Vol. 1 pp. 265-274, 1989.

Author Profile

Tae-Hyun Chang

He was educated at Dong-A University (B.E, 1969, M.E. 1971) in Korea. After obtaining his B.E. he was worked at Busan Thermal Power Plant(Korea Electric Company) for 10 years as a mechanical engineer. He obtained his PhD. at the department of mechanical engineering of the University of Wales (Swansea, UK) in 1991. He has been working for Kyungnam University since 1978 at the division of mechanical and automation engineering. He was promoted to a professor and appointed the dean of evening school for two years in 1998. He worked as a chairman of ASV'6 at Korea on May 28 - 31 2001. His major research fields are convection heat transfer with and without swirl in a tube. He has published five text books and more than 90 research papers.